ARTICLE

Efficient Electron Transfer in Functional Assemblies of Pyridine-Modified NQDs on SWNTs

Sohee Jeong,[†,§,*] Hyung Cheoul Shim,[†,‡,§] Soohyun Kim,[‡] and Chang-Soo Han[†,*]

[†]Nanomechanical Systems Research Division, Korea Institute of Machinery and Materials (KIMM), Daejeon 305-343, Korea, and [‡]School of Mechanical, Aerospace & Systems Engineering, Department of Mechanical Engineering, Korea Advanced Institute of Science and Technology (KAIST) 373-1, Daejeon 305-343, Korea. [§]These authors contributed equally to this work.

ABSTRACT Nanocrystal quantum dot (NQD)/single-walled carbon nanotube (SWNT) hybrid nanomaterials were synthesized, assembled into field effect transistors (FETs) *via* dielectrophoresis (DEP), and characterized optically and electronically. The pyridine moiety functioned as a short, noncovalent linker between the NQDs and SWNTs and allowed more efficient carrier transfer through the assemblies without deleteriously altering electronic structures. Photoluminescence studies of the resulting assemblies support an efficient carrier transfer process in CdSe-*py*-SWNTs unlike that of CdSe/ZnS-*py*-SWNTs. The use of DEP as a means of controlling the assembly process allowed the creation of a SWNT array containing densely packed CdSe NQDs across a 2 μm gap between electrodes. Observations and characterization of the photocurrent, resistivity, gate dependence, and optical properties of these systems suggest efficient electron transfer from photoexcited NQDs to SWNTs.

KEYWORDS: 0D−1D hybrid · CdSe nanocrystal quantum dot · single-walled carbon nanotube · noncovalent adsorption · carrier transfer · photoluminescence · photocurrent

Semiconductor nanocrystal quantum dots (NQDs) have recently attracted considerable interest for use in optoelectronic applications.[1−3] NQDs are solution processable and can be synthesized using colloidal routes, allowing their band gaps to be tuned over a considerable range by varying the particle size. Recent advancements in multiple-exciton generation in NQD solutions have afforded possible efficiency improvements in photovoltaic devices.[4−6] Despite these advantages, the use of NQDs in optoelectronic applications has been limited due to poor transport properties when they are assembled into two-dimensional (2D) structures.[7]

The ability to transport extracted carriers from NQDs is essential for the development of most NQD-based applications. Strategies to facilitate carrier transport while preserving optical characteristics have included (1) the fabrication of neat NQD films with modified surfaces by attaching ligands or by applying physical processes such as heat annealing[7−9] and (2) coupling NQDs to one-dimensional (1D) nanostructures such as single-walled carbon nanotubes (SWNTs) or various types of nanowires.[10−12] NQD−nanowire hybrid nanostructures are expected to facilitate selective wavelength absorption, charge transfer to 1D nanostructures, and efficient carrier transport. Recently, Leschkies *et al.*[13] demonstrated the attachment of CdSe NQDs to the surface of substrate-grown ZnO nanowires using carboxylate linkers.

SWNTs are one of the most widely explored 1D building block structures and have demonstrated an emerging potential in nanoscale devices due to their unique properties, including small size, large aspect ratio, large current carrier density, and ballistic transport properties.[14] For these reasons, SWNTs have been considered as channels in nanoscale transistors.[14−19] Efforts have been made to fabricate devices from NQD−SWNT composite materials in which the SWNTs form a channel where the movement of charge carriers transferred from the NQD component can take place.[10,20,21] Despite the interest in using NQD−SWNT hybrid materials in optoelectronic applications, no reports have clearly elucidated their optoelectronic behavior when assembled in FETs due to the complexity involved in the preparation and characterization of both components.

In the present study, the optical properties of both NQDs and SWNTs were monitored through synthesis, assembly, and device fabrication. More importantly, by using pyridine molecules as a noncovalent linker, the resulting assemblies were made with precise density control and without deleteriously altering the electronic structures. The degree of photoluminescence quenching in CdSe-*py*-SWNTs supports the formation of a nonradiative decay pathway upon

*Address correspondence to sjeong@kimm.re.kr, cshan@kimm.re.kr.

Received for review August 11, 2009 and accepted December 15, 2009.

Published online December 22, 2009. 10.1021/nn9009938

assembly. Systems containing CdSe and those containing CdSe/ZnS differ in the extent of photoluminescence quenching. The charge transfer mechanisms in these systems were investigated by measuring electrical signals from aligned NQD-*py*-SWNT FETs assembled using dielectrophoresis (DEP).

RESULTS AND DISCUSSION

Assembly of NQD-*py*-SWNTs: The light-absorbing building blocks, made up of CdSe core and CdSe/ZnS core/shell NQDs, were synthesized according to standard literature procedures with slight modifications.[22,23] These building blocks are among the most well-studied NQD systems with regard to both synthesis and characterization, and their band gaps can be easily tuned over the entire visible range. As prepared, the NQDs were passivated with trioctylphosphine, oleyl amine, and oleic acid and dispersed in a nonpolar solvent such as toluene. The surface of the NQDs was modified with linker molecules to create an assembled structure. SWNTs were chosen to act as a conduit for carrier exchange with NQDs because of their unique electrical and ballistic electron transport properties.

Both SWNTs and NQDs are easily functionalized through both covalent and noncovalent modification,[10−12] and many routes toward the creation of NQD−SWNT assemblies have been explored. To form NQD−SWNT assemblies suitable for light collection and carrier transfer, an appropriate linker molecule must be carefully chosen based on the following criteria: (1) the electronic properties of the linked materials must be maintained throughout the entire process; (2) the linker must be functionalized such that it can bind to both components; and (3) the distance between the NQD and SWNT should be as short as possible to enhance the efficiency of electron tunneling.[13]

On the basis of these criteria, pyridine was chosen as the linker moiety to attach CdSe or CdSe/ZnS NQDs to SWNTs. Note that the electronic structure of NQDs is sensitive to the surface attachment of other molecules, especially when the nanoparticles are not epitaxially coated with a large band gap material such as ZnS. For example, small, thiol-containing molecules, which are widely used for functionalizing NQD surfaces, can create a hole trap and result in charged NQDs.[24] Also, in CdSe NQDs, light-induced disulfide bond formation can be detrimental to stability. In contrast, pyridine molecules, when exchanged with insulating ligands on the nanocrystal surface, are known to passivate the surface state. Furthermore, when fabricated in 2D arrays, the conductivity of the NQD film is enhanced.[25]

Replacing the hydrophobic alkyl tail of the as-synthesized NQD with an aromatic pyridine tail allows the nanocrystals to be noncovalently bound to the SWNT *via* $\pi-\pi$ stacking interactions. This adsorptive attachment retains the electronic properties of the SWNT. Covalent attachment of NQDs to SWNTs achieved through oxidation of the SWNT to form carboxyl functionalities on the nanotube surface tends to disrupt the π-bonding system of the sp^2-hybridized orbitals and creates defects. As a consequence, the conductivity and other electrical properties of SWNTs are strongly affected.[22]

Although noncovalent attachment preserves the electronic structures of SWNTs, large linker molecules are not suitable for creating hybrid nanostructures that rely on "*photon absorption and transportation*".[26] A short linker group is preferred, such as pyridine or any other small, conjugated alkene.

As described in Figure 1a, the NQD surface was exchanged with excess pyridine and attached to SWNTs by sonication. The resulting solutions were filtered through a Microcon Ultracel filter (MWCF 1 000 000 Da, Fisher Scientific) to remove unbound NQDs. The electronic structures of both components were preserved throughout the assembly process, as confirmed by absorption and Raman spectra (Figure 1b,d, respectively). More specifically, the G peak near 1590 cm^{-1} in the Raman spectrum, which represents the unique carbon bonding of SWNTs, did not shift or distort after pyridine attachment. Figure 1b shows that the absorption spectra of pyridine-modified CdSe NQDs dispersed in chloroform showed no substantial differences when compared to the optical transition of CdSe prepared in toluene. The quantum-confined 1S optical transition can be seen at approximately 522 nm. TEM images indicate an average diameter of 2.8 nm.

The ratio of NQDs to SWNTs was varied to ensure that the assemblies contained the large amount of NQDs. The optical density of the assembly, measured at 400 nm (CdSe) and 808 nm (SWNT), was used as a measure of the number of NQDs per SWNT.[27,28] No 1S transitions were observed with only a 10-fold excess of NQDs (data not shown), possibly due to the low density of CdSe NQDs adsorbed on the SWNTs. The use of a 100- or 1000-fold excess of NQDs resulted in a clearly visible 1S transition (Figure 1b). Figure 1c shows typical TEM images of the CdSe-*py*-SWNT hybrid nanostructures at different magnifications. The images obtained on structures formed with a 100-fold excess of CdSe reveal the adsorption of a large number of CdSe NQDs with diameters of about 2.8 nm onto the surface of the SWNTs.

Photoluminescence Quenching in CdSe-*py*-SWNTs: As previously observed by several research groups that have examined NQD−carbon nanotube (CNT) assemblies,[20,22,26] the CdSe-*py*-SWNT nanoassemblies exhibited photoluminescence (PL) quenching of CdSe (Figure 1e, inset). PL quenching in CdSe−CNT is generally considered as being due to the introduction of alternative nonradiative decay pathways. Interestingly, the PL of CdSe/ZnS decreased slightly upon association with SWNTs (Figure 1e, TEM images in Supporting Information). In previous studies, CdSe/CdS core/shell par-

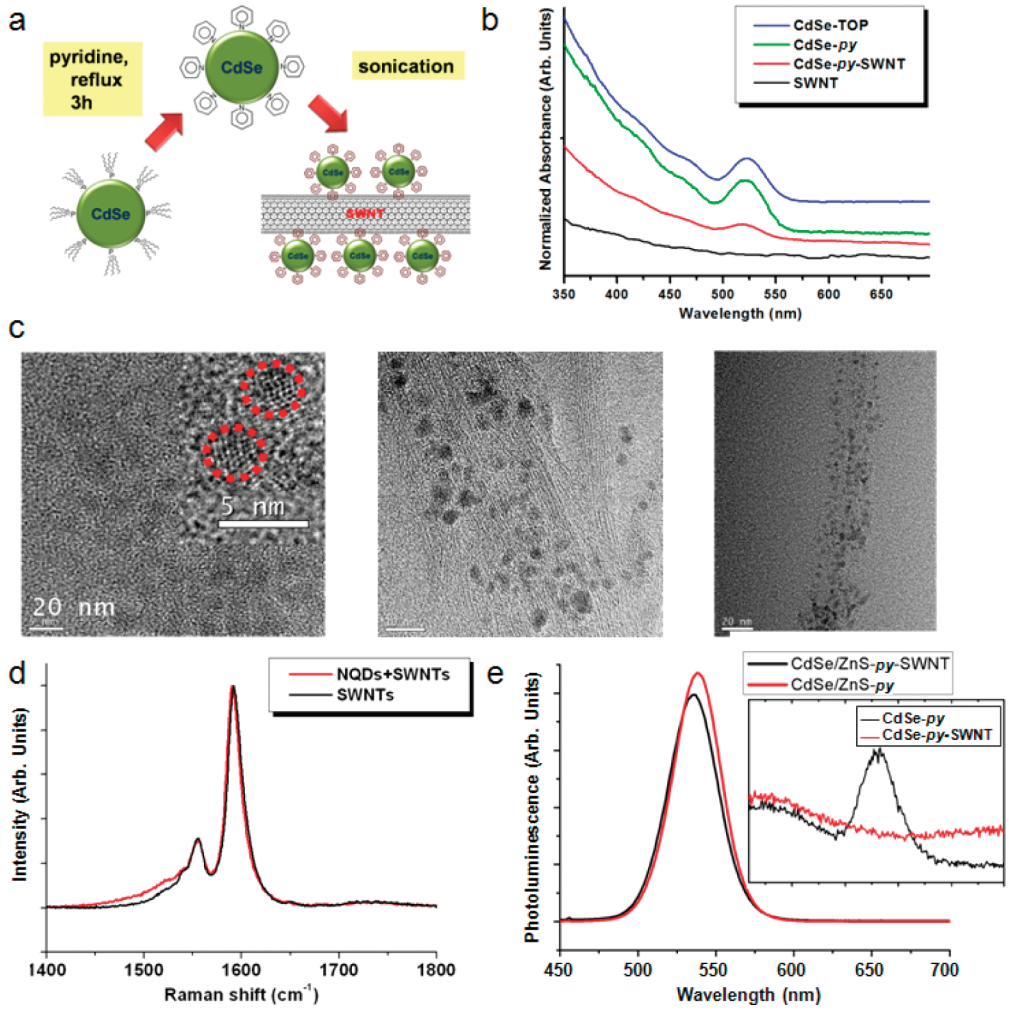

Figure 1. (a) Schematic diagram illustrates the noncovalent approach used to fabricate the NQD−SWNT hybrid structures. (b) UV/vis absorption spectra show the optical transitions of synthesized CdSe particles prior to surface modification (trioctylphosphine-capped CdSe in toluene), CdSe-*py*, CdSe-*py*-SWNT hybrid nanostructure, and SWNT. The 1S transition of CdSe at 522 nm was retained throughout the process. (c) TEM images show the CdSe nanocrystals (left, average size ~2.8 nm) and the hybrid CdSe-*py*-SWNT (middle and right). (d) Raman spectra of SWNTs (black line) and CdSe-*py*-SWNTs (red line). (e) Emission spectra of CdSe (inset) and CdSe/ZnS are shown before and after attachment to SWNTs.

ticles were attached to multiwalled carbon nanotubes, resulting in near complete PL quenching.[22] CdS has a smaller band gap, and the conduction band offsets between CdSe are smaller (~0.32 eV) and therefore more susceptible to PL quenching. It has also been observed that if the shell coating is not sufficiently thick charge carriers may leak from the core.[29] Under these circumstances, charge transport properties are easily influenced by the surface state of the particle. The ZnS shell used in the current study has a larger band gap and may confine the exciton more efficiently, thereby resulting in a slight decrease in PL intensity.

Possible pathways for nonradiative decay have been identified as (1) electron transfer from NQDs to SWNTs, (2) hole transfer from NQDs to SWNTs, and (3) resonant energy transfer. On the basis of the energy level diagram in Figure 2, photoexcitation results in electron−hole separation and both carriers are amenable to transfer. The conduction and valence band levels for both CdSe nanocrystals and SWNTs depend on their diameter and occur at 3.5 and 5.5 eV in 2.8 nm diameter CdSe nanocrystals[30,31] and at 4.8 and 5.4 eV in SWNTs,[32] respectively. Because the effective mass of a hole ($1.19m_e$, where m_e is the electron mass)[30] in CdSe is much larger than the effective mass of an electron ($0.11m_e$),[30] the valence energy in CdSe NQDs does not change, while the conduction energy changes noticeably. The identity of the primary carrier in the NQD−SWNT device was determined by measuring various electrical signals of the NQD−SWNT assemblies.

Photocurrents in CdSe-*py*-SWNT FETs. CdSe-*py*-SWNT assemblies were fabricated into FETs using DEP (Figure 3a) to monitor the electrical signatures upon NQD photoexcitation and to investigate the mechanism of charge transfer. Details of device fabrication can be found in the Supporting Information. As indicated, only semiconducting SWNTs were used in this experiment. An n-doped silicon substrate was used as the back gate, and the aligned CdSe-*py*-SWNT hybrid nanostructures were deposited between microelectrodes to function as

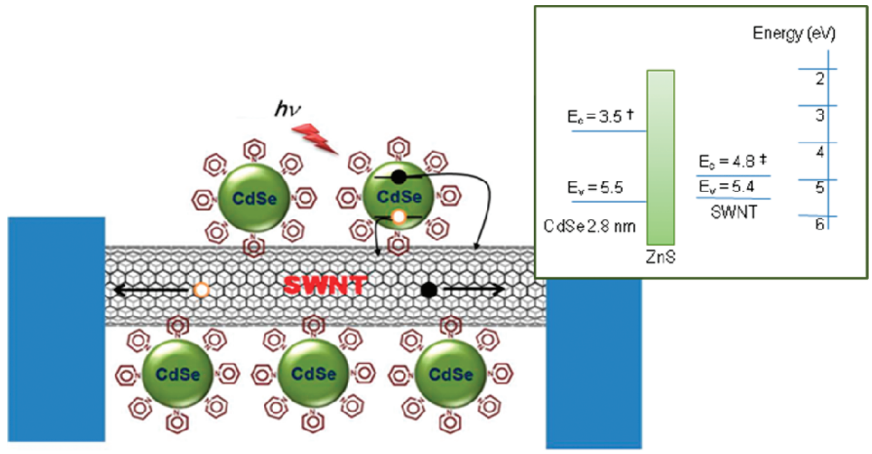

Figure 2. Energy diagram is given for the CdSe core (†)[32] and the CdSe/ZnS core/shell with respect to that of semiconducting SWNTs (‡)[31] (inset).

the channel in the FET structure. The CdSe-*py*-SWNT device was packaged into a conventional chip using wire bonding. The resistance between the source and drain within the fabricated FET was measured in real time with a bias voltage of 100 mV using a digital multimeter (189, Fluke Corp., Everett, WA). As shown in Figure 3b, the resistance decreased when illuminated and increased when the light was off. The light source consisted of a conventional UV lamp with an intensity of 1.2 mW/cm^2 (*I*) at an excitation wavelength of 365 nm (VL-6.LC, Vilber Lourmat, Cedex, France).

The resistance changes upon illumination are a result of charge transfer from NQDs to SWNTs. More specifically, once excitons were created by light absorption, charge carriers (electrons or holes or both) were transferred to the SNWTs, with a flow toward the oppositely charged electrode.

Therefore, more current was generated when the light was on, causing a decrease in the apparent resistance. The resistance was also measured during illumination at two different excitation wavelengths: 365 and 254 nm. The resistance as a function of wavelength is shown in Figure 3c, where the rate of change in resistance was less with the longer excitation wavelength and may be a result of lower absorption. The current−voltage curve (Figure 3d) shows a slight increase (~370 nA) in current at 0 V when illuminated, which also supports the idea of carrier transfer to SWNTs upon illumination. In contrast, the resistance of "SWNT only" devices increased upon illumination due to molecular desorption effects in the pristine SWNT.[33]

In previous studies, FETs formed by CdSe−SWNT hybrid nanostructures have shown contradictory results, with an increase in resistivity upon illumination. This ob-

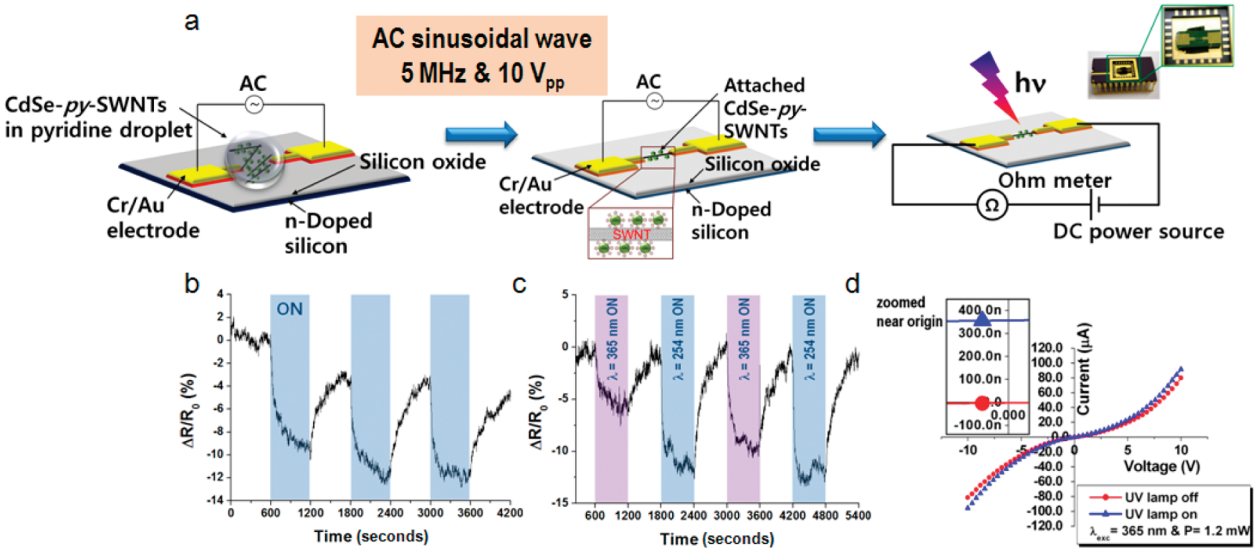

Figure 3. (a) Schematic diagrams show the dielectrophoretic assembly and the electrical measurement techniques. An ac voltage (5 MHz, 10 V_{pp}) was applied across the electrodes. (b) Resistance of a CdSe-*py*-SWNT FET device was monitored as a function of time under a small applied bias (V_{ds}) of 100 mV, I = 1.2 mW/cm^2, and λ = 365 nm. (c) Resistance when illuminated was determined at different wavelengths. (d) Current *versus* voltage sweep curve was recorded in the absence of incident light (red circles) and under UV irradiation (blue triangles).

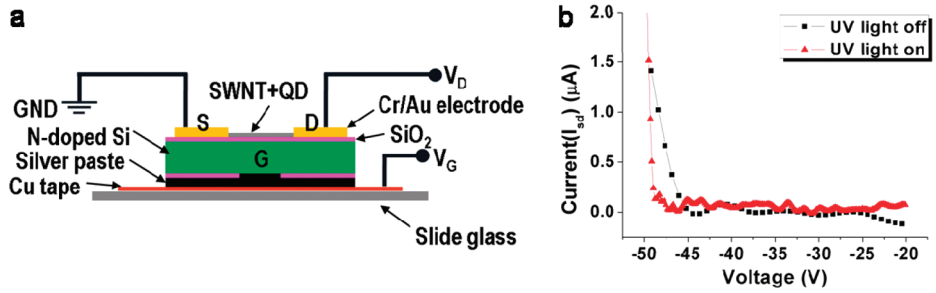

Figure 4. (a) Schematic diagram shows the configuration of a CdSe-*py*-SWNT FET for measurements of gate dependence. (b) Gate dependence curve of a CdSe-*py*-SWNT FET is shown with illumination on and off; λ = 365 nm, *I* = 1.2 mW/cm².

servation was accounted for by electron transfer from the photoexcited NQDs to the SWNTs, thereby reducing the number of holes.[20] Conversely, Jeong *et al.*[21] observed an increase in photocurrent induced by carrier transfer from CdSe/ZnS NQDs when they were fabricated into FETs with an individual SWNT. Although the exact nature of the signal was not identical in these two cases (resistivity and current, respectively), opposing results were obtained regarding the photoexcitation of NQDs. The magnitude of the response in the NQD−SWNT system was dependent on whether the SWNTs were aligned or networked. However, the same trend in photoresponse should be derived regardless of the morphology of the SWNT assembly as long as the contact resistance of the device is controlled.[30] Therefore, the discrepancies in the above studies most likely stemmed from the fact that, in the networked system, the NQD density was low (15:1-fold excess,[20] not specified in Jeong *et al.*'s article[21]) relative to that in the single SWNT−FET system. In the case of low-density NQD coverage, the electrons transferred from the NQDs likely played a role in compensating the existing hole carriers. The current system differs in that the number of NQDs attached to a single SWNT ranged from 10 to 1000. FET experiments were performed using hybrid materials synthesized with a 100-fold excess of NQDs. The short pyridine linker group may also facilitate more efficient carrier transfer, based on complete PL quenching, even with a 10-fold excess of NQDs.

Carrier Transfer Mechanism: The efficiency of charge transfer is determined not only by the energy difference between donor (CdSe) and acceptor (SWNT) but also by the exciton binding energy of the NQDs. The donor−acceptor energy difference should be greater than the exciton binding energy of CdSe, which is relatively large (over 0.1 eV) in a quantum-confined system.[31] This large exciton binding energy of CdSe and the relatively small effective mass of electrons may account for the observed electron transfer from NQDs to SWNTs.

The gate dependence characteristics in these CdSe-*py*-SWNT FET devices using the system illustrated in Figure 4a strongly supports this hypothesis. Undoped SWNTs are p-type semiconducting materials[17] with holes as the majority charge carrier. When a negative voltage was applied, the CdSe-*py*-SWNT FET switched to an on-state due to the accumulation of holes between the source and drain. Conversely, the application of a positive voltage results in a dramatic switch to the off-state. Figure 4b shows a typical gate characteristic curve (black squares) of an aligned CdSe-*py*-SWNT FET. The gate characteristic curve shifts to the left (red triangles) upon illumination. Because electrons are the primary carriers in this system and are transferred from CdSe to SWNTs, the hole concentration inside the SWNT decreased, resulting in a shift of the threshold voltage in the transfer curve to the left, as shown in Figure 4b.

Additionally, no changes in resistivity were observed upon illumination of a core/shell-*py*-SWNT FET (Supporting Information, Figure S2). Both optical and electronic measurements support the hypotheses that (1) the photocurrent is a result of carrier transfer from photoexcited NQDs to SWNTs and (2) in the core/shell system, the electron and hole created upon light absorption recombine radiatively, while carriers in the core-only system were transferred to the SWNT.

In summary, NQD−SWNT FET systems were fabricated and demonstrated efficient charge transfer from photoexcited NQDs to SWNTs. Despite the current interest in using SWNTs as 1D building blocks for carrier transport, their narrow band gap, which allows transfer of both holes and electrons, may complicate the electrical behavior of optoelectronic hybrid devices based on SWNT nanostructures. The current study differs from previous attempts to fabricate efficient NQD−SWNT FET systems by employing noncovalent interactions to preserve the electronic structure of both components (NQD and SWNT) and by aligning relatively few SWNT molecules between electrodes as opposed to using a networked SWNT film and elucidated a carrier transfer mechanism dominated by electron transfer. This allowed the determination of the charge carrier mechanism at the interface of 0D−1D hybrid nanostructures through (1) careful ligand choice to preserve the properties of both 0D and 1D materials, (2) characterization of the hybrid structures by TEM and optical spectroscopy, and (3) monitoring the electrical signal and gate

dependence. Further research on fabricating photovoltaic devices using this NQD−SWNT hybrid nanostructure is currently underway.

EXPERIMENTAL SECTION

Chemicals: Oleylamine, oleic acid, pyridine, diethyl zinc (1 M solution in heptane), hexamethyldisilathiane, and squalane were purchased from Sigma-Aldrich (St. Louis, MO) and used as received without further purification. Trioctylphosphine (TOP) was purchased from Sigma-Aldrich and degassed prior to use. Selenium shot and cadmium 2,4-pentanedionate were purchased from Alfa Aesar (Ward Hill, MA). TOP/selenide stock solutions, either 1.0 or 1.5 M, were prepared in a glovebox by stirring TOP and selenium shot overnight. All chemicals were stored in an inert atmosphere glovebox prior to use.

High-pressure CO conversion (HiPCO) SWNTs were purchased from Carbon Nanotechnologies Inc. (CNI, Houston, TX) with a purity of approximately 70%. The average diameter of an SWNT was 1 nm, with an average length of about 1 μm.

Synthesis and Surface Modification of Nanocrystal Quantum Dots: CdSe and CdSe/ZnS nanocrystal quantum dots were prepared using established colloidal synthetic techniques as described in the literature with a few modifications.[22,23] Briefly, CdSe/ZnS core−shell nanoparticles capped with a mixture of trioctylphosphine, oleyl amine, and oleic acid ligands were prepared using a stepwise procedure that consisted of CdSe core growth, heterogeneous ZnS shell growth, and particle annealing.

Constructing SWNT−NQD Hybrid Nanostructures: After extensive washing to remove excess growth ligands, NQDs were surface-ligand exchanged with pyridine by stirring overnight with mild heating. An excess of pyridine molecules (over 10× the calculated mol % of surface atoms) was used to complete the surface exchange. The resulting NQDs were precipitated using acetone. Pyridine-modified NQDs were then mixed with SWNT powder and sonicated until optically clear solutions were obtained (bath type sonicator, 40 kHz, 5−10 min). The solutions were then filtered through a a Microcon Ultracel filter (MWCF 1 000 000 Da, Fisher Scientific, Pittsburgh, PA) to remove unbound NQDs. Solutions with precise ratios of NQDs to SWNTs were prepared by varying the ratio from 10 to 10 000. Concentrations of NQDs were calculated by measuring the optical density at 400 nm.[27]

Device Fabrication: SWNT−NQD solution concentrations and the volume of droplets were fixed at 1.3 μg/mL (based on the amount of SWNT) and 0.2 μL, respectively, considering the size of the microelectrode plate area. The microelectrode plate was fabricated by conventional photolithography. Silicon oxide was deposited as an insulating layer to a height of 100 nm on the n-doped silicon substrate by thermal oxidation. The Cr/Au electrode was deposited onto the silicon oxide to a height of 50 nm using chemical vapor deposition (CVD). The gap between the microelectrodes was about 2 μm, with an electrode width of 5 μm.

Dielectrophoresis Assembly of SWNT−NQD: The dielectrophoresis apparatus consisted of two elements: an approaching element and an inducing element. The approaching element was composed of two probes with Cr/Au microelectrodes as counter electrodes. To support the sample device, a holder was fixed to the *z*-axis of a translational stage. The two probes apply a voltage to each electrode through a conventional function generator (Agilent, 33220A), and each probe could be adjusted using an *xyz* stage. The inducing element of the apparatus was composed of a signal generator with an oscilloscope (54602B, Hewlett-Packard, Palo Alto, CA) as the signal detector. An ac electric field was generated and monitored with the oscilloscope. After switching the function generator to sinusoidal wave mode with amplitude of 10 V_{pp} and a frequency of 5 MHz, a drop of the NQD-*py*-SWNT suspension was applied to the microelectrode gap with a micropipet. The sinusoidal wave was applied to the microelectrodes until the droplet dried completely, which typically took about 1 min. The function generator was then turned off. The device was then heat-annealed at 300 °C for 30 s to reduce the resistance. Only functioning devices were selected for photocurrent measurements. Further details are given in the Supporting Information.

Spectroscopic Characterization: Room-temperature optical absorption spectra were collected on an SD-1000 spectrometer (Scinco Inc., Seoul, Korea) using 1 cm quartz or glass cuvettes. Photoluminescence (PL) measurements were performed on a Fluorolog-3 spectrometer (HORIBA Jobin Yvon Inc., Edison, NJ) at room temperature with a 1 nm slit width on both excitation and emission monochromators.

Photocurrent Measurements: Device resistance was measured using a digital multimeter (189, Fluke Corp.), and real-time data were acquired through FlukeView software. An ultraviolet (UV) lamp (6 W, peak emission λ_p = 365 nm) was used as the light source. The distance from the light source to the device was fixed at 5 cm (~1.2 mW/cm^2 at the device). Other electrical properties were measured using a Keithley model 2400 (Keithley, Cleveland, OH).

Gate Characteristics: The gate voltage effect was measured using a source meter (Keithley 2400). Silicon oxide was deposited as an insulating layer at a thickness of 10 nm, and an n-doped silicon substrate was used as the back gate. The drain bias was set to 100 mV.

Acknowledgment. This research was supported by the Nano R&D program through the Korea Science and Engineering Foundation funded by the Ministry of Education, Science and Technology (Grant 2009-0083219) and 21C Frontier Research Program from the Center for Nanoscale Mechantronics and Manufacturing. H.C. Shim acknowledges a financial support by the Ministry of Knowledge Economy (MKE) and Korea Institute for Advancement in Technology (KIAT) through the Workforce Development Program in Strategic Technology and the second stage of the Brain Korea 21 Project in 2008.

Supporting Information Available: Details of device preparation and the resistance characteristics of a CdSe/ZnS-*py*-SWNT FET device are provided. This material is available free of charge *via* the Internet at http://pubs.acs.org.

REFERENCES AND NOTES

1. Huynh, W. U.; Peng, X.; Alivisatos, A. P. CdSe NSanocrystal Rods/Poly(3-hexylthiophene) Composite Photovoltaic Devices. *Adv. Mater.* **1999**, *11*, 923–927.
2. Coe, S.; Woo, W. K.; Bawendi, M.; Bulovic, V. Electroluminescence from Single Monolayers of Nanocrystals in Molecular Organic Devices. *Nature* **2002**, *420*, 800–803.
3. Konstantatos, G.; Howard, I.; Fischer, A.; Hoogland, S.; Clifford, J.; Klem, E.; Levina, L.; Sargent, E. H. Ultrasensitive Solution-Cast Quantum Dot Photodetectors. *Nature* **2006**, *442*, 180–183.
4. Schaller, R. D.; Klimov, V. I. High Efficiency Carrier Multiplication in PbSe Nanocrystals: Implications for Solar Energy Conversion. *Phys. Rev. Lett.* **2004**, *92*, 186601.
5. Ellington, R. J.; Beard, M. C.; Johnson, J. C.; Yu, P.; Micic, O. I.; Nozik, A. J.; Shabaev, A.; Efros, A. L. Highly Efficient Multiple Exciton Generation in Colloidal PbSe and PbS Quantum Dots. *Nano Lett.* **2005**, *5*, 865–871.
6. Kim, S. J.S; Kim, W. J.; Sahoo, Y.; Cartwright, A. N.; Prasad, P. N. Multiple Exciton Generation and Electrical Extraction from a PbSe Quantum Dot Photoconductor. *Appl. Phys. Lett.* **2008**, *92*, 031107.
7. Yu, D.; Wang, C.; Guyot-Sionnest, P. n-Type Conducting CdSe Canocrystal Solids. *Science* **2003**, *300*, 1277–1280.
8. Porter, V. J.; Geyer, S.; Halpert, J. E.; Kastner, M. A.; Bawendi, M. G. Photoconduction in Annealed and Chemically Treated CdSe/ZnS Inorganic Nanocrystal Films. *J. Phys. Chem. C* **2008**, *112*, 2308–2316.
9. Jarosz, M. V.; Porter, V. J.; Fisher, B. R.; Kastner, M. A.; Bawendi, M. G. Photoconductivity Studies of Treated CdSe Quantum Dot Films Exhibiting Increased Exciton Ionization Efficiency. *Phys. Rev. B: Condens. Matter* **2004**, *70*, 1–12.
10. Ravindran, S.; Chaudhary, S.; Colburn, B.; Ozkan, M.; Ozkan, C. S. Covalent Coupling of Quantum Dots to Multiwalled Carbon Nanotubes for Electronic Device Applications. *Nano Lett.* **2003**, *3*, 447–453.

11. Ravindran, S.; Bozhilov, K. N.; Ozkan, C. S. Self Assembly of Ordered Artificial Solids of Semiconducting ZnS Capped CdSe Nanoparticles at Carbon Nanotube Ends. *Carbon* **2004**, *42*, 1537–1542.
12. Landi, B. J.; Evans, C. M.; Worman, J. J.; Castro, S. L.; Bailey, S. G.; Raffaelle, R. P. Noncovalent Attachment of CdSe Quantum Dots to Single Wall Carbon Nanotubes. *Mater. Lett.* **2006**, *60*, 3502–3506.
13. Leschkies, K. S.; Divakar, R.; Basu, J.; Enache-Pommer, E.; Boercker, J. E.; Carter, C. B.; Kortshagen, U. R.; Norris, D. J.; Aydil, E. S. Photosensitization of ZnO Nanowires with CdSe Quantum Dots for Photovoltaic Devices. *Nano Lett.* **2007**, *7*, 1793–1798.
14. Avouris, P.; Appenzeller, J.; Martel, R.; Wind, S. J. Carbon Nanotube Electronics. *Proc. IEEE* **2003**, *91*, 1772–1784.
15. Durkop, T.; Getty, S.; Cobas, E.; Further, M. Extraordinary Mobility in Semiconducting Carbon Nanotubes. *Nano Lett.* **2004**, *4*, 35–39.
16. Javey, A.; Guo, J.; Wang, Q.; Mand, L.; Dai, H. Ballistic Carbon Nanotube Field-Effect Transistors. *Nature* **2003**, *424*, 654–657.
17. Martel, R.; Schmidt, T.; Shea, H. R.; Hertel, T.; Avouris, P. Single- and Multi-wall Carbon Nanotube Field-Effect Transistors. *Appl. Phys. Lett.* **1998**, *73*, 2447–2449.
18. Martel, R.; Wong, H. S.; Chan, K.; Avouris, P. Carbon Nanotube Field Effect Ttransistors for Logic Applications. *Proc. IEDM* **2000**, 159–161.
19. Tan, S.; Verschueren, A.; Dekke, C. Room-Temperature Transistor Based on Single Carbon Nanotubes. *Nature* **1998**, *393*, 49–52.
20. Hu, L.; Zhao, Y.-L.; Ryu, K.; Zhou, C.; Stoddart, J. F.; Grüner, G. Light-Induced Charge Transfer in Pyrene/CdSe−SWNT Hybrids. *Adv. Mater.* **2008**, *20*, 939–946.
21. Jeong, S. Y.; Lim, S. C.; Bae, D. J.; Lee, Y. H.; Shin, H. J.; Yoon, S.-M.; Choi, J. Y.; Cha, O. H.; Jeong, M. S.; Perello, D.; Yun, M. Photocurrent of CdSe Nanocrystals on Single-Walled Carbon Nanotube-Field Effect Transistor. *Appl. Phys. Lett.* **2008**, *92*, 243103.
22. Olek, M.; Bu1sgen, T.; Hilgendorff, M.; Giersig, M. Quantum Dot Modified Multiwall Carbon Nanotubes. *J. Phys. Chem. B* **2006**, *110*, 12901–12904.
23. Yen, B. K.; Gunther, A.; Schmidt, M. A.; Jensen, K. F.; Bawendi, M. G. A Microfabricated Gas−Liquid Segmented Flow Reactor for High-Temperature Synthesis: The Case of CdSe Quantum Dots. *Angew. Chem., Int. Ed.* **2005**, *44*, 5447–5451.
24. Jeong, S.; Achermann, M.; Nanda, J.; Ivanov, S.; Klimov, V. I.; Hollingsworth, J. A. Effect of the Thiol−Thiolate Equilibrium on the Photophysical Properties of Aqueous CdSe/ZnS Nanocrystal Quantum Dots. *J. Am. Chem. Soc.* **2005**, *127*, 10126–10127.
25. Leatherdale, C. A.; Kagan, C. R.; Morgan, N. Y.; Empedocles, S. A.; Kastner, M. A.; Bawandi, M. G. Photoconductivity in CdSe Quantum Dot Solids. *Phys. Rev. B* **2000**, *62*, 2669–2680.
26. Li, Q.; Sun, B.; Kinloch, I. A.; Zhi, D.; Sirringhaus, H.; Windle, A. H. Enhanced Self-Assembly of Pyridine-Capped CdSe Nanocrystals on Individual Single-Walled Carbon Nanotubes. *Chem. Mater.* **2006**, *18*, 164–168.
27. Leatherdale, C. A.; Woo, W. K.; Mikulec, F. V.; Bawendi, M. G. On the Absorption Cross Section of CdSe Nanocrystal Quantum Dots. *J. Phys. Chem. B* **2002**, *106*, 7619–7622.
28. Kam, N. W. S.; O'Connell, M.; Widson, J. A.; Dai, H. Carbon Nanotubes as Multifunctional Biological Transporters and Near-Infrared Agents for Selective Cancer Cell Destruction. *Proc. Natl. Acad. Sci. U.S.A.* **2005**, *102*, 11600–11605.
29. Dabbousi, B. O.; Rodriguez-Viejo, J.; Mikulec, F. V.; Heine, J. R.; Mattoussi, H.; Ober, R.; Jensen, K. F.; Bawendi, M. G. (CdSe)ZnS Core−Shell Quantum Dots: Synthesis and Characterization of a Size Series of Highly Luminescent Nanocrystallites. *J. Phys. Chem. B* **1997**, *101*, 9463–9475.
30. Efros, A. L.; Rosen, M. The Electronic Structure of Semiconductor Nanocrystals. *Annu. Rev. Mater. Sci.* **2000**, *30*, 475–521.
31. Kucur, E.; Qu, L.; Riegler, G. A.; Urban, G. A.; Nann, T. Determination of Quantum Confinement in CdSe Nanocrystals by Cyclic Voltammetry. *J. Chem. Phys.* **2003**, *119*, 2333–2337.
32. Kazaoui, S.; Minami, N.; Matsuda, N. Electrochemical Tuning of Electronic States in Single-Wall Carbon Nanotubes Studied by *In Situ* Absorption Spectroscopy and AC Resistance. *Appl. Phys. Lett.* **2001**, *78*, 3433–3435.
33. Chen, R. J.; Franklin, N. R.; Kong, J.; Cao, J.; Tombler, T. W.; Zhang, Y.; Dai, H. Molecular Photodesorption from Single-Walled Carbon Nanotubes. *Appl. Phys. Lett.* **2001**, *79*, 2258–2260.